

Study of the isospin structure of single-pion production in charged-current neutrino interactions

N. J. Baker, A. M. Cnops,* P. L. Connolly, S. A. Kahn, M. J. Murtagh, R. B. Palmer, N. P. Samios, and M. Tanaka
Brookhaven National Laboratory, Upton, New York 11973

(Received 12 November 1980)

The isospin structure of weak single-pion production in the reactions $\nu p \rightarrow \mu^- p \pi^+$, $\nu n \rightarrow \mu^- p \pi^0$, and $\nu n \rightarrow \mu^- n \pi^+$ has been studied using the 7-foot deuterium bubble chamber exposed to a wide-band neutrino beam at BNL. We find that the $I = 1/2 N\pi$ amplitude is substantial even in the $\Delta(1232)$ mass region and the relative phase angle ψ is approximately 90° as predicted by the Adler model.

I. INTRODUCTION

Weak charged-current one-pion production processes have been extensively studied in the past, both from the theoretical and the experimental points of view. In particular, $\Delta(1232)$ production has been considered in the framework of isobar models¹ in which the dominant role of the Δ resonance characterizes the $I = \frac{3}{2}$ amplitude of the reactions.

This paper gives the results of our isospin analysis of the following charged-current (CC) reactions:

$$\nu_\mu p \rightarrow \mu^- p \pi^+, \quad (1)$$

$$\nu_\mu n \rightarrow \mu^- p \pi^0, \quad (2)$$

$$\nu_\mu n \rightarrow \mu^- n \pi^+. \quad (3)$$

The corresponding scattering amplitudes (excluding isotensor exchange) are given by

$$\text{Amp}(\mu^- p \pi^+) = A_{3/2}, \quad (4)$$

$$\text{Amp}(\mu^- p \pi^0) = \frac{1}{3} \sqrt{2} (A_{3/2} - A_{1/2}), \quad (5)$$

$$\text{Amp}(\mu^- n \pi^+) = \frac{1}{3} (A_{3/2} + 2A_{1/2}), \quad (6)$$

where the reduced isovector amplitudes $A_{3/2}$ and $A_{1/2}$ correspond to the $I = \frac{3}{2}$ and $I = \frac{1}{2} N\pi$ systems, respectively. If the $N\pi$ systems were all pure $I = \frac{3}{2}$ states, then the relative cross-section ratios would be

$$\sigma(\mu^- p \pi^+) : \sigma(\mu^- p \pi^0) : \sigma(\mu^- n \pi^+) = 9 : 2 : 1.$$

We find the ratio of the amplitudes $\eta = |A_{1/2}| / |A_{3/2}| = 0.60 \pm 0.07$ and the relative phase angle $\psi = 90^\circ \pm 11^\circ$ in the mass region $M_{N\pi} < 1.4$ GeV. There are two other experiments which have measured the values of η and ψ in the same mass region: one with the ANL 12-foot deuterium chamber² ($\eta = 0.57 \pm 0.06$, $\psi = 89.2^\circ \pm 8.7^\circ$), the other with the Gargamelle (GGM) heavy-liquid chamber³ at the CERN PS ($\eta = 0.71 \pm 0.14$ and $\psi = 75^{+12}_{-16}^\circ$). Our results are in good agreement with the 12-foot results and are

also consistent with the predictions of the Adler model for weak one-pion production.⁴

II. EXPERIMENTAL DETAILS

The data were obtained from an analysis of 1 000 000 pictures taken in the BNL 7-foot deuterium bubble chamber. Details of the experiment are discussed elsewhere.⁵ The chamber was exposed to a broad-band neutrino beam whose energy spectrum peaked at 1 GeV. The film was scanned for neutral-induced interactions (≥ 2 prongs). Each event was measured and processes through the TVGP kinematic program and then reexamined by physicists. To remove scatters due to incoming charged particles and to minimize any possible scanning and/or measuring biases, the events within a fiducial volume of 4 m³ were accepted only if the total visible momentum $|\vec{P}_{\text{vis}}|$ was greater than 300 MeV/c and the angle θ_{vis} between \vec{P}_{vis} and the beam direction was less than 50° . In addition any events which fitted to an incoming charged-particle-scatter hypothesis were rejected from the sample. CC events were required to have at least one negative track which left the bubble chamber or underwent a $\mu^- \rightarrow e^-$ decay. After these cuts 3300 CC events remained from an initial sample of 6400 events. About a quarter of the film was rescanned and the single-scanning efficiency was greater than 88%.

The selection of events for reactions (1), (2), and (3) is based on kinematic fitting and particle identification. Since the neutrino-beam direction is known to 0.5° , a three-constraint (3C) fit can be performed for $\nu p \rightarrow \mu^- p \pi^+$. In the kinematic fitting the standard bubble-chamber method is used for assigning an initial value of 0 ± 45 MeV/c to the momentum components of the spectator neutron in the deuteron nucleus. The event assignment to reaction (1) is unique except that we lose events with a high-momentum spectator neutron (≥ 120 MeV/c). The selection of events for reactions (2) and (3) is not as straightforward since there is an undetected neutral particle in the final

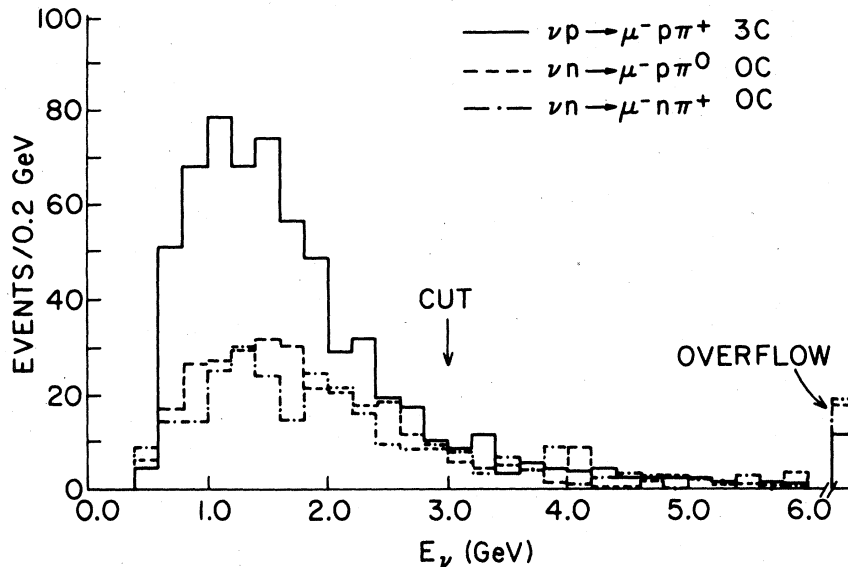


FIG. 1. The distributions in neutrino energy E_ν for the final states $\mu^- p \pi^+$, $\mu^- p \pi^0$, and $\mu^- n \pi^+$. For the isospin analysis, events with $E_\nu < 3.0$ GeV are used.

states. There is also complexity caused by ambiguities between the recoil proton and the spectator proton. We therefore selected only two-prong events. Since protons with momentum greater than ~ 120 MeV/ c are measurable in this experiment, the use of two-prong events is equivalent to rejecting events with a fast spectator proton. If one assumes that the spectator momentum distribution is the same for all three reactions then the selection procedures ensure that the event losses for all reactions are the same. From studying the 3C-fit $\nu d \rightarrow \mu^- p p_s$ events the correction for this loss is estimated to be $(25 \pm 4)\%$ and it is common for all three reactions. Therefore, this correction does not affect the following analysis. For the selected events we attempted 0C fits to reaction (2) and (3) hypotheses. The kinematical ambiguities between $\mu^- p \pi^0$ and $\mu^- n \pi^+$ final states are, in general, resolved by the visual and measured track information. The remaining ambiguous events (about 16%) are weighted by $\frac{1}{2}$ and assigned to both reactions. By comparing the ambiguous events with the unique events, we find that this procedure introduces a negligible bias in the isospin analysis of the $\Delta(1232)$ mass region ($M_{N\pi} \lesssim 1.4$ GeV).

The possible biases to reactions (2) and (3) are carefully examined by using the 3C $\nu p \rightarrow \mu^- p \pi^+$ events, eliminating an appropriate charged track from the event, then simulating the $\mu^- p$, $\mu^- p \pi^0$, and $\mu^- n \pi^+$ final states. We find that $(12 \pm 2)\%$ of the $\mu^- n \pi^+$ events are lost by the visible-angle cut $\theta_{\text{vis}} < 50^\circ$ and $(8 \pm 3)\%$ of the $\mu^- p \pi^0$ are misclassified

as 3C $\mu^- p$ events. The main source of background for reactions (2) and (3) is contamination from the multipion production channels. The magnitude of the contamination is estimated by studying the 3C $\nu n \rightarrow \mu^- p \pi^+ \pi^-$ and $\nu p \rightarrow \mu^- p \pi^+ \pi^+ \pi^-$ samples and it is found to be strongly dependent upon the incident neutrino energy. To minimize contamination from this source without losing many events, we select only one-pion events with $E_\nu < 3.0$ GeV for the isospin analysis (see Fig. 1). With this cut the estimated contamination is about 15% while only 20% of the good events are removed. Other sources of background are the neutral-current (NC) $\nu n \rightarrow \nu p \pi^-$, $\nu n \pi^+ \pi^-$ and the neutron-induced reactions $nn \rightarrow n p \pi^-$, $nn \pi^+ \pi^-$ where the π^- leaves the chamber without interacting. From the observed NC candidates and the known π^- detection efficiency we calculate this background to be $(11 \pm 2)\%$ in the $\mu^- p \pi^0$ sample and $(6 \pm 2)\%$ in the $\mu^- n \pi^+$ sample. Finally the correction for $(13 \pm 2)\%$ hydrogen contamination in the deuterium is applied for the $\mu^- p \pi^+$ sample.

TABLE I. The observed number of events and the corrected number of events for the single-pion reactions.

Reaction Fit	$E_\nu < 3.0$ GeV		
	$\mu^- p \pi^+$ 3C	$\mu^- p \pi^0$ 0C	$\mu^- n \pi^+$ 0C
Selected	554	267	217
Corrected	482 ± 25	218 ± 16	198 ± 15
$M_{N\pi} < 1.6$ GeV	468 ± 24	185 ± 14	168 ± 13
$M_{N\pi} < 1.4$ GeV	466 ± 24	133 ± 12	119 ± 11

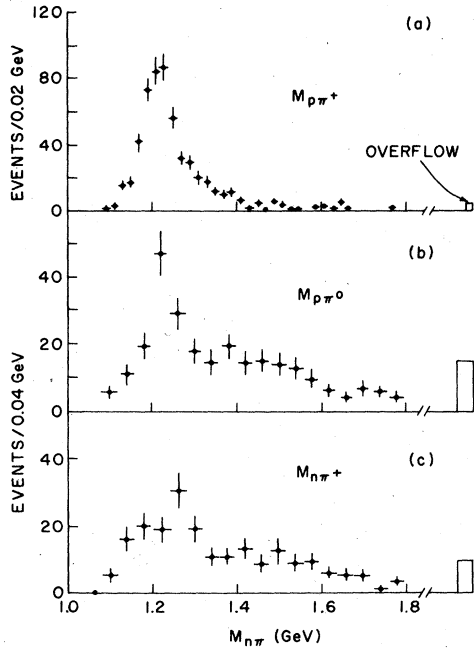


FIG. 2. The distributions of the $N\pi$ invariant-mass $M_{N\pi}$ for the single-pion final states.

III. RESULTS

The observed number of events for reactions (1), (2), and (3) and the number after making corrections for background and biases are summarized in Table I. The $N\pi$ invariant-mass $M_{N\pi}$ distributions are shown in Fig. 2. In Fig. 2(a) clear $\Delta^*(1232)$ production is seen with a negligible number of events at high mass in the $\mu^-p\pi^+$ final state. In Figs. 2(b) and 2(c) the $\Delta^*(1232)$ production is no longer dominant but still clearly visible in the $\mu^-p\pi^0$ state and there is evidence for production of high-mass $N\pi$ states in the 1.4–1.8 GeV mass region. The $I = \frac{1}{2}$ amplitude must be responsible for this broad enhancement since from Fig. 2(a) the $I = \frac{3}{2}$ amplitude is small for $M_{N\pi} \gtrsim 1.5$ GeV. Figure 3 shows the four-momentum-transfer-squared Q^2 distributions.

Using the corrected number of events in each

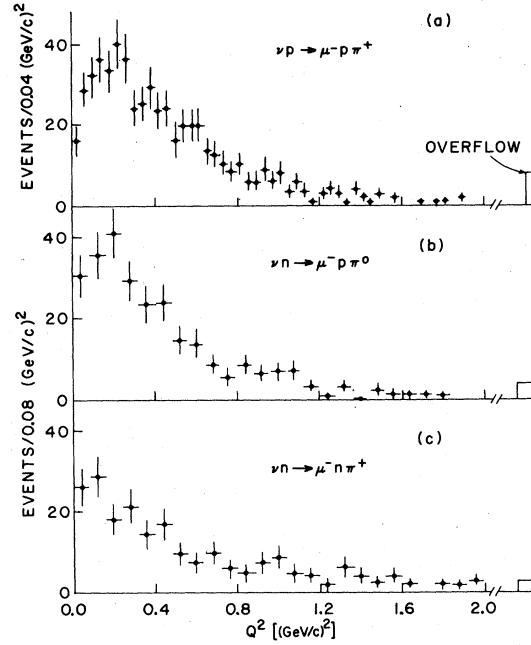


FIG. 3. The distributions in four-momentum transfer squared Q^2 for the single-pion final states.

reaction, we can deduce two independent ratios of cross sections

$$R_1 = \frac{\sigma(\mu^-p\pi^0)}{\sigma(\mu^-p\pi^+)}, \quad R_2 = \frac{\sigma(\mu^-n\pi^+)}{\sigma(\mu^-p\pi^+)},$$

which can then be interpreted in term of $\eta = |A_{1/2}|/|A_{3/2}|$ and the relative phase ψ . The results for various $M_{N\pi}$ cuts are summarized in Table II and plotted in Fig. 4 together with the PS GGM (Ref. 3) and the ANL 12-foot results.² The quoted errors in Table II and Fig. 4 are statistical only. The systematic errors, mainly due to the correction for contamination from the multipion production channels, are estimated to be the same order of the statistical errors at most. For $M_{N\pi} < 1.4$ GeV, we find that the $A_{1/2}$ amplitude is comparable to the $A_{3/2}$ amplitude ($\eta = 0.60 \pm 0.07$) and on average the $A_{3/2}$ and $A_{1/2}$ amplitudes are almost exactly 90° out of phase ($\psi = 90^\circ \pm 11^\circ$), where

TABLE II. Results.

	$M_{N\pi} < 1.4$ GeV	$M_{N\pi} < 1.6$ GeV	Total
$R_1 = \sigma(\mu^-p\pi^0)/\sigma(\mu^-p\pi^+)$	0.30 ± 0.03	0.39 ± 0.04	0.45 ± 0.04
$R_2 = \sigma(\mu^-n\pi^+)/\sigma(\mu^-p\pi^+)$	0.27 ± 0.03	0.36 ± 0.03	0.41 ± 0.04
$\eta = A_{1/2} / A_{3/2} $	0.60 ± 0.05	0.79 ± 0.05	0.89 ± 0.05
Relative phase angle ψ	$90^\circ \pm 8^\circ$	$95^\circ \pm 7^\circ$	$97^\circ \pm 6^\circ$

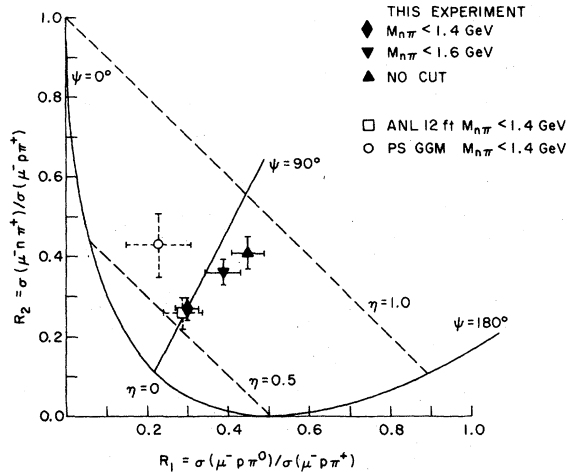


FIG. 4. Plot of the cross-section ratios $R_1 = \sigma(\mu^- p \pi^0) / \sigma(\mu^- p \pi^+)$ and $R_2 = \sigma(\mu^- n \pi^+) / \sigma(\mu^- p \pi^+)$. The dashed straight lines and the solid lines correspond to equal values of $\eta = |A_{1/2}| / |A_{3/2}|$ and the relative phase angle ψ , respectively. \blacktriangle this experiment; \blacktriangledown this experiment, $M_{N\pi} < 1.6$ GeV; \blacklozenge this experiment, $M_{N\pi} < 1.4$ GeV. The results of the GGM and the 12-foot-chamber experiments are also shown.

the errors include systematic effects. This is consistent with the postulate that in the $\Delta(1232)$ resonance region the $A_{3/2}$ phase varies to π from zero ($\pi/2$ at the resonance), while that of the nonresonance amplitude $A_{1/2}$ remains close to zero.⁶ Our values are in good agreement with

TABLE III. Comparison of Adler's theoretical predictions with the 7-foot results.

	$M_{N\pi} < 1.4$ GeV	
	η	ψ
Basic model	0.69	93°
Extended model I	0.58	88°
Extended model II	0.58	92°
This experiment	0.60 ± 0.05	$90^\circ \pm 8^\circ$

the 12-foot results ($\eta = 0.57 \pm 0.06$, $\eta = 89.2^\circ \pm 8.7^\circ$) but are in poorer agreement with the GGM results ($\eta = 0.71 \pm 0.14$, $\psi = 75^{+12}_{-16}^\circ$), although the beam spectra and experimental cuts differ between experiments. We also find that the contribution of the $A_{1/2}$ amplitude increases with the $M_{N\pi}$ mass but the phase angle ψ stays close to 90° . The data agree well with Adler's theoretical predictions⁴ for the 7-foot experiment, especially with the values of the extended models as seen in Table III.

ACKNOWLEDGMENTS

We would like to thank the AGS staff, crews of the 7-foot chamber, and the scanning and measuring groups at BNL whose efforts made this experiment possible. This work was supported by the U. S. Department of Energy under Contract No. DE-AC02-76CH00016.

*Present address: DD Division, CERN, Geneva Switzerland.

¹For example, see the review paper of C. H. Llewellyn Smith, Phys. Rep. **32**, 261 (1972).

²V. E. Barnes *et al.*, in *Neutrino-78*, Proceedings of the International Conference on Neutrino Physics and Astrophysics, Purdue Univ., 1978, edited by E. C. Fowler (Purdue University Press, West LaFayette,

Indiana, 1978), p. C56. See also S. J. Barish *et al.*, Phys. Rev. D **19**, 2521 (1979).

³M. Pohl *et al.*, Lett. Nuovo Cimento **24**, 540 (1979).

⁴S. L. Adler, Ann. Phys. (N.Y.) **50**, 189 (1968); Phys. Rev. D **12**, 2644 (1975).

⁵N. J. Baker *et al.*, Phys. Rev. D **23**, 2499 (1981).

⁶L. M. Sehgal, Report No. ANL-HEP-PR-75-45 (unpublished), pp. 23-25.